Fault behavior of a wave energy converter: a benchmark model development

Erica Michelle Lindbeck

Office of Science, Science Undergraduate Laboratory Internship Program

University of Central Florida, Orlando, FL

National Renewable Energy Laboratory

Golden, Colorado

August 9, 2019

Prepared in partial fulfillment of the requirement of the Department of Energy, Office of Science's Science Undergraduate Laboratory Internship Program under the direction of Nathan Tom at the National Renewable Energy Laboratory.

Participant: Erica Lindbeck
Erica Lindbeck

Research Advisor: Nathan Tom
Nathan Tom

ABSTRACT

In this paper models of faulty wave energy converter (WEC) components are developed in the open source modeling platform, WEC-Sim. Two of these faulty component models are then applied to a point absorber WEC model with basic controller damping and driving forces. Resulting changes in device behavior are recorded as a benchmark for the development of future condition monitoring and fault-tolerant control systems, and possible explanations for some of the observed trends are provided. The paper concludes with possible directions of future research in terms of additional fault models and applications.

I. INTRODUCTION

Wave energy converters (WECs) face many challenges on the path to commercial viability. Most difficulties arise from the irregularity in size, frequency, and direction of incoming waves. In unfavorable conditions, such as during hurricanes, a device may experience loads up to one hundred times the average for the location[1], making damage to the device extremely likely. Given the novelty of the technology, very little reliability data is known, and most is estimated from other industries or from manufacturer's data.[2] Repairing a damaged device poses its own challenges, as offshore locations may only be accessible periodically due to tidal and wave conditions. Condition monitoring coupled with fault-tolerant or adaptive control systems may be able to dramatically increase the availability of WECs as well as their efficiency during faults.

To design such systems, appropriate models of wave energy converters under fault conditions must be developed. There is little consensus on a specific design for WECs,[1] so a modelling method which can be adapted to a wide variety of device types is desired. WEC-Sim[3] is an open-source MATLAB/Simulink-based simulation platform which can be used to model WEC devices that consist of rigid bodies, joints, power take-off (PTO) systems, and mooring systems, as well as sensors and controllers. Faults which affect these components are likely to have similar realizations in all WECs. Thus, in this study, fault modules are developed to simulate electrical and mechanical faults of common components. These fault modules are then applied to a model of a Wavestar[4]-like point absorber WEC to determine their effects on performance. Controller parameters and sea states are varied for each fault to generate a benchmark data set for future reference in fault-tolerant controller design.

II. FAULT MODELING

Simulink models for four electrical faults and three mechanical faults were developed for use with WEC-Sim.

A. Electrical faults

As WEC-Sim's PTO blocks are simple, generator faults could not be modeled with great accuracy. Thus, the focus of this study was on sensor faults. The most common sensor faults are predicted based on experience in the aerospace[5] and wind energy[6] sectors, as well as several real-world data sets that were analyzed for fault prevalence.[7] The sensor faults are implemented by the addition of a MATLAB function block within the controller block of the WEC's Simulink model. The function block takes the non-faulty signals as input, then passes fault-injected signals to the relevant controller input ports. The physical mechanism by which a fault occurs is not modeled, as this is dependent on the sensor type and the fault model is meant to be as general and adaptable as possible.

1. Bias and drift

A bias fault is a constant offset to the true signal with time. A drift fault is a varying offset to the true signal, and for this study the offset is linearly increasing in magnitude in accordance with Balaban et al.[5] Thus, fault injection into the signal x at time t is accomplished by

$$x_{fault}(t) = x(t) + b + d * t \tag{1}$$

where b = bias and d = drift.

2. Noise

A noise fault is an excessive amount of noise present in a signal. For this study gaussian white noise is injected to a signal x at time t by

$$x_{fault}(t) = x(t) + \sigma * randn(t) \tag{2}$$

where σ is the standard deviation of the noise and $randn(t)$ is a random value from a normal distribution at time t.

3. Scaling

A scaling fault is a scalar multiplication of the true signal by some constant value. Thus, fault injection is modeled by

$$x_{fault}(t) = S * x(t) \tag{3}$$

where S is the scaling factor.

4. Dropouts

A dropout fault is a jump to a predetermined constant value for a brief period. For this study, the pre-determined value was set to 0. A probability of dropout was also pre-determined, represented as a decimal value, p. At each time step, a random number from a uniform distribution on (0,1) was generated, and if less than p,

$$x_{fault}(t) = 0 \tag{4}$$

Otherwise the signal was passed unchanged.

B. Mechanical faults

Common mechanical faults are predicted based on discussion with wave energy researchers, as well as fault analysis from both wave[8] and offshore wind[9] energy sectors. They are implemented by substituting a component model with additional fault-induced force or torque for the non-faulty component model.

1. Jammed hinge

A hinge may become jammed by debris or marine biofouling, reducing freedom of movement. To model this behavior, a WEC-Sim rotational constraint block is replaced by the WEC-Sim rotational PTO block, which is functionally identical when the damping coefficient is set to 0 but allows the addition of an input torque. An input torque is then applied representing the increased friction of a jammed hinge, and is composed of Stribeck, Coulomb, and viscous components. This friction torque is pulled from the MATLAB Rotational Friction block in the form of

$$T_{friction} = \sqrt{2e}(T_{brk} - T_c) * \exp\left(-\left(\frac{\omega}{\omega_{St}}\right)^2\right) * \frac{\omega}{\omega_{St}} + T_c * \tanh\left(\frac{\omega}{\omega_{Coul}}\right) + f\omega \tag{5}$$

where

T_{brk} = breakaway friction torque
T_c = Coulomb friction torque
ω = relative velocity
ω_{St} = $\omega_{brk}\sqrt{2}$ = Stribeck velocity threshold
ω_{brk} = breakaway friction velocity
ω_{Coul} = $\omega_{brk}/10$ = Coulomb velocity threshold
f = viscous friction coefficient

2. Fixed joint wear

A fixed joint may become weakened over time by impacts and fatigue, becoming effectively a hinge with a high coefficient of friction. This is easily modeled by replacing the fixed constraint block with a rotational PTO block with friction as input torque, as detailed in the previous section.

3. Bearing wear

Linear PTOs developed for use in WECs typically experience high attractive forces between the translator and stator, which must by counteracted by bearings. These bearings are subject to fatigue and failure, effectively increasing friction between the translator and stator. This is modeled by adding an input force representing the increased friction, and is composed of Stribeck, Coulomb, and viscous components. This friction force is pulled from the MATLAB Translational Friction block in the form of

$$F_{friction} = \sqrt{2e}(F_{brk} - F_c) * \exp\left(-\left(\frac{v}{v_{St}}\right)^2\right) * \frac{v}{v_{St}} + F_c * \tanh\left(\frac{v}{v_{Coul}}\right) + fv \quad (6)$$

where

F_{brk} = breakaway friction
F_c = Coulomb friction
v = relative velocity
v_{St} = $\omega_{brk}\sqrt{2}$ = Stribeck velocity threshold
v_{brk} = breakaway friction velocity
v_{Coul} = $\omega_{brk}/10$ = Coulomb velocity threshold
f = viscous friction coefficient

III. FAULT APPLICATION

A. Device model

The Wavestar-like WEC model used in this study for the generation of performance data is the single degree of freedom (DOF) device used in the WEC Control Competition (WECCCOMP)[10] for optimal control system design. The Simulink model and the physical device are shown in Figure 1.

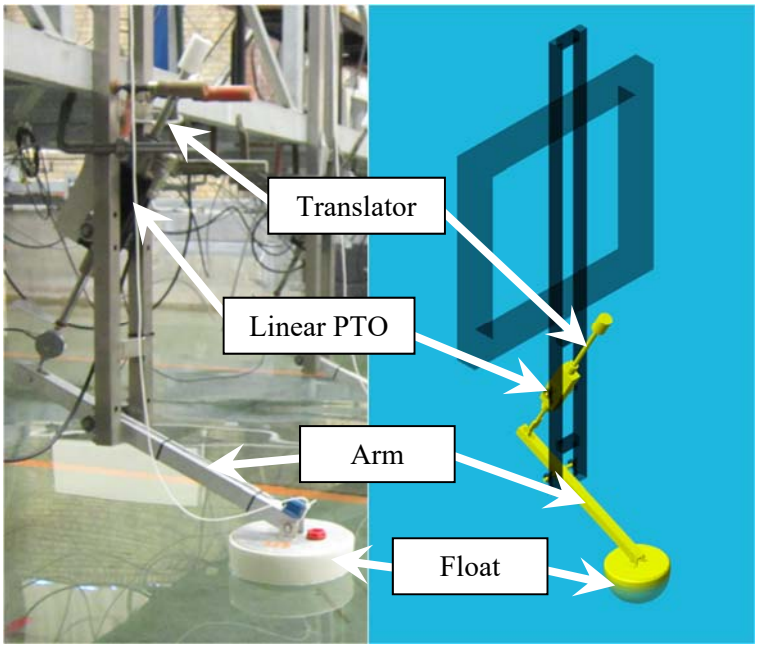

FIG. 1. Wavestar-like WEC. Physical device being modeled (left). Simulink model (right).

The WEC consists of a float fixed to the end of an arm, which in turn is connected to the translator of a linear PTO. The rotation of the arm as the float bobs in the waves induces linear oscillatory motion in the translator, which leads to electrical generation by the PTO. An accelerometer measures the motion of the float and a displacement sensor measures that of the translator. The net force on the translator is also measured. The PTO controller commands an output force $F_{controller} = cv + kx$ that is a combination of a damping force, cv, to absorb power and a forcing term/spring force, kx, to force the float's motion to better match the oscillation frequency of the incoming waves. Translator position x is given by the position sensor, and the translator velocity signal v is derived by the application of a differentiator and low pass filter to the position signal.

B. Condition variation

To observe trends in WEC behavior during faults, a range of controller parameters and wave conditions were applied. Controller damping (c) was varied from 1 Ns/m to 20 Ns/m, and the controller forcing term's spring constant (k) was varied from -5 N/m to -100 N/m. The WEC was simulated in six irregular wave states generated by JONSWAP spectra, detailed in Table 1, using the same seed. A complete set of combinations of these parameters and conditions was tested for a baseline state, a position signal bias fault, and a position signal scaling fault. The position bias varied with sea state, with a bias of +0.005 in sea states 1 and 4, +0.007 in sea states 2 and 5, and +0.05 in sea states 3 and 6. The scaling fault involved a scaling factor of 1.15 in all wave states. In the baseline cases, as well as in the fault cases, some small amplitude white

noise ($\sigma = 0.0015$) and a low probability of dropout (3%) were added to the position signal as they could be expected even in a properly calibrated sensor.

Table 1. Wave states applied to the WEC

Wave State	γ	Significant Wave Height (m)	Significant Wave Period (s)
1	1.0	0.0208	0.988
2	1.0	0.0625	1.412
3	1.0	0.1042	1.836
4	3.3	0.0208	0.988
5	3.3	0.0625	1.412
6	3.3	0.1042	1.836

C. Performance evaluation

To evaluate the performance of the WEC under varying fault conditions, wave states, and control parameters, the performance criterion developed for WECCCOMP was used. This performance criterion, ρ, is calculated by the equation

$$\rho = \frac{avg(P)}{2 + \frac{|f|_{98}}{F_{max}} + \frac{|z|_{98}}{Z_{max}} - \frac{avg|P|}{|P|_{98}}} \tag{7}$$

where

$avg(P)$ = average absorbed electrical power
$|f|_{98}$ = 98th percentile of absolute force
F_{max} = force constraint (60 N)
$|z|_{98}$ = 98th percentile of absolute displacement
Z_{max} = displacement constraint (0.08 m)
$avg|P|$ = mean absolute electrical power magnitude
$|P|_{98}$ = 98th percentile of absolute power

The performance criterion has units of watts and is proportional to the average absorbed power, so that a negative value is returned if power is, on average, consumed by the device instead of absorbed. Other than increased average power absorption, performance is considered to increase with decreases in translator forces and displacement (reducing device fatigue), and as average absorbed power approaches 98th percentile absorbed power (corresponding to more uniform power absorption over time). As the performance criterion can vary greatly from absorbed power, to avoid confusion, performance criterion units will be neglected for the rest of this work.

It is worth noting that average absorbed electrical power and mean power magnitude are based on the electrical power output of the PTO, while 98th percentile of absolute power is based on the mechanical power input to the PTO. This means PTO efficiency is a factor in the performance criterion, although it is maintained at 70% throughout this study. It should also be noted that the force and displacement constraints are not applied to the PTO model directly, so that the translator may experience forces and displacements greater than those constraints during the simulation, indicating that a more robust PTO could achieve better performance.

IV. RESULTS & DISCUSSION

A. Performance trends

The performance criterion for each combination of wave state and controller parameters was recorded for the baseline, position sensor signal bias fault, and position sensor signal scaling fault conditions. The results for wave state 6, limited to positive performance, are provided in Figures 2-4 as a representative example. A sample of the faulty position sensor signals for the scaling and bias fault cases are given in Figures 5 and 6, respectively.

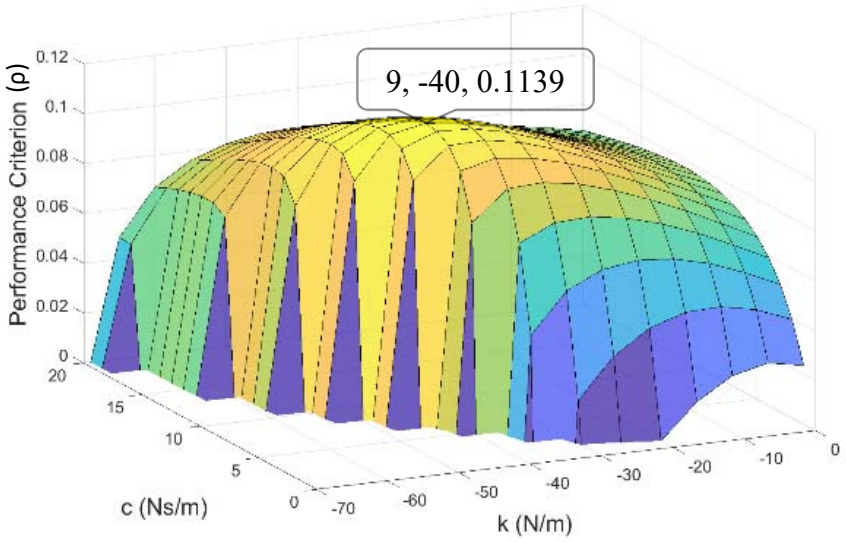

FIG 2. Baseline WEC performance in wave state 6

For a fixed damping coefficient or spring constant, performance decreases gradually as the other parameter is increased from the optimum value and decreases sharply as the other parameter is decreased from the optimum value.

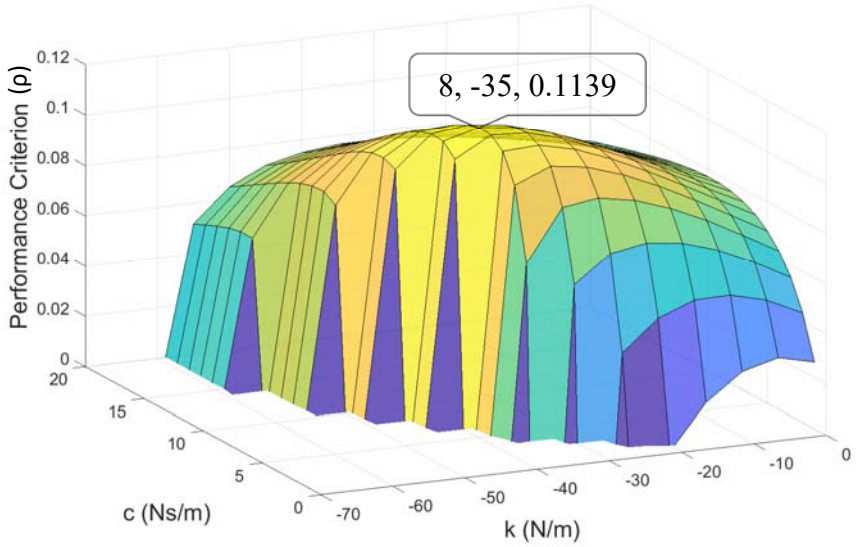

FIG 3. WEC performance during position sensor signal scaling fault in wave state 6

The same trends in performance are observed during the scaling fault as in the baseline case, and the same maximum performance is obtained. However, the maximum performance is obtained at lower magnitude controller parameters than in the baseline case.

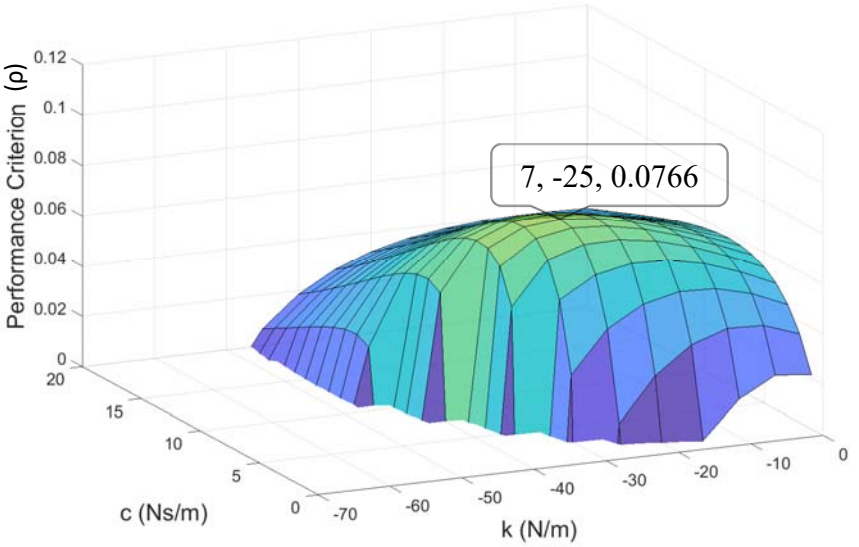

FIG 4. WEC performance during position sensor signal bias fault in wave state 6

The same trends in performance are observed during the bias fault as in the baseline case, but the same maximum obtainable performance is reduced by 32.7%. Further, the new maximum performance is obtained at significantly smaller magnitude controller parameters than in the baseline, while at the parameters which are optimum in the baseline case, the performance is reduced by 53.7% from the baseline performance.

B. Device behavior trends

The elements of device behavior which contribute to performance, such as average absorbed power, 98^{th} percentile force, and 98^{th} percentile displacement, were recorded in addition to the overall performance criterion. Representative examples of these trends as well as the trends in performance for wave state 6 are given in Figure 7 and 8.

During a scaling fault, at low magnitude damping and spring coefficients, greater power absorption is observed than in the baseline, which is desirable, but 98^{th} percentile forces and displacements are also greater, which is undesirable. With the specific formulation of the performance criterion, the result is higher overall performance at low damping and spring coefficients. Similarly, lower power absorption and 98^{th} percentile displacement are observed at high magnitude damping and spring coefficients, although the 98^{th} percentile force is still greater than in baseline, for an overall reduced performance.

During a bias fault, all factors contributing to the performance criterion trend in an undesirable direction. The largest change occurs in the 98^{th} percentile displacement at high magnitude controller parameters, while the largest consistent change across parameter values is in the 98^{th} percentile power.

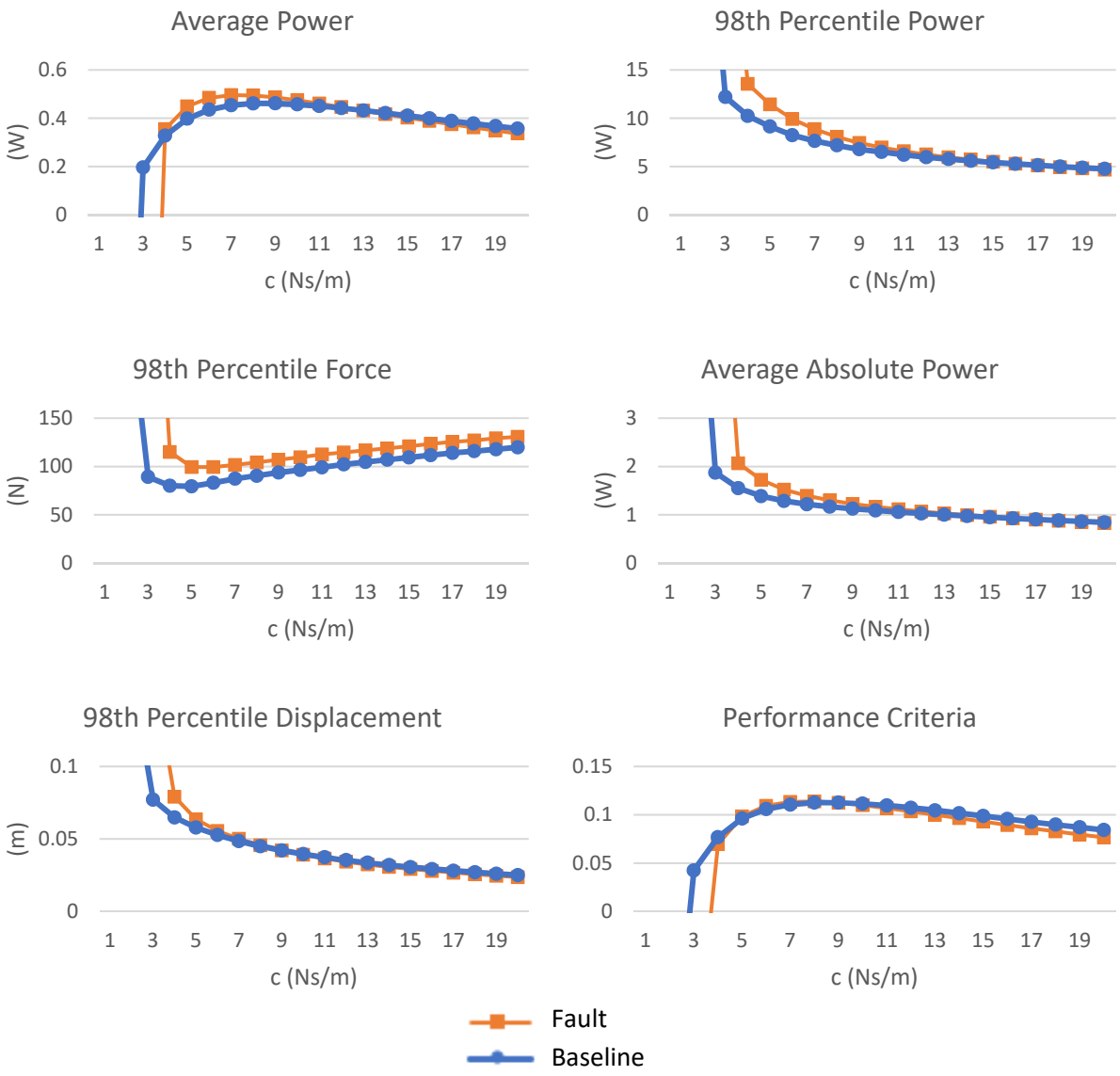

FIG 7. Behavior trends for k = -35 N/m during position sensor signal scaling fault in wave state 6

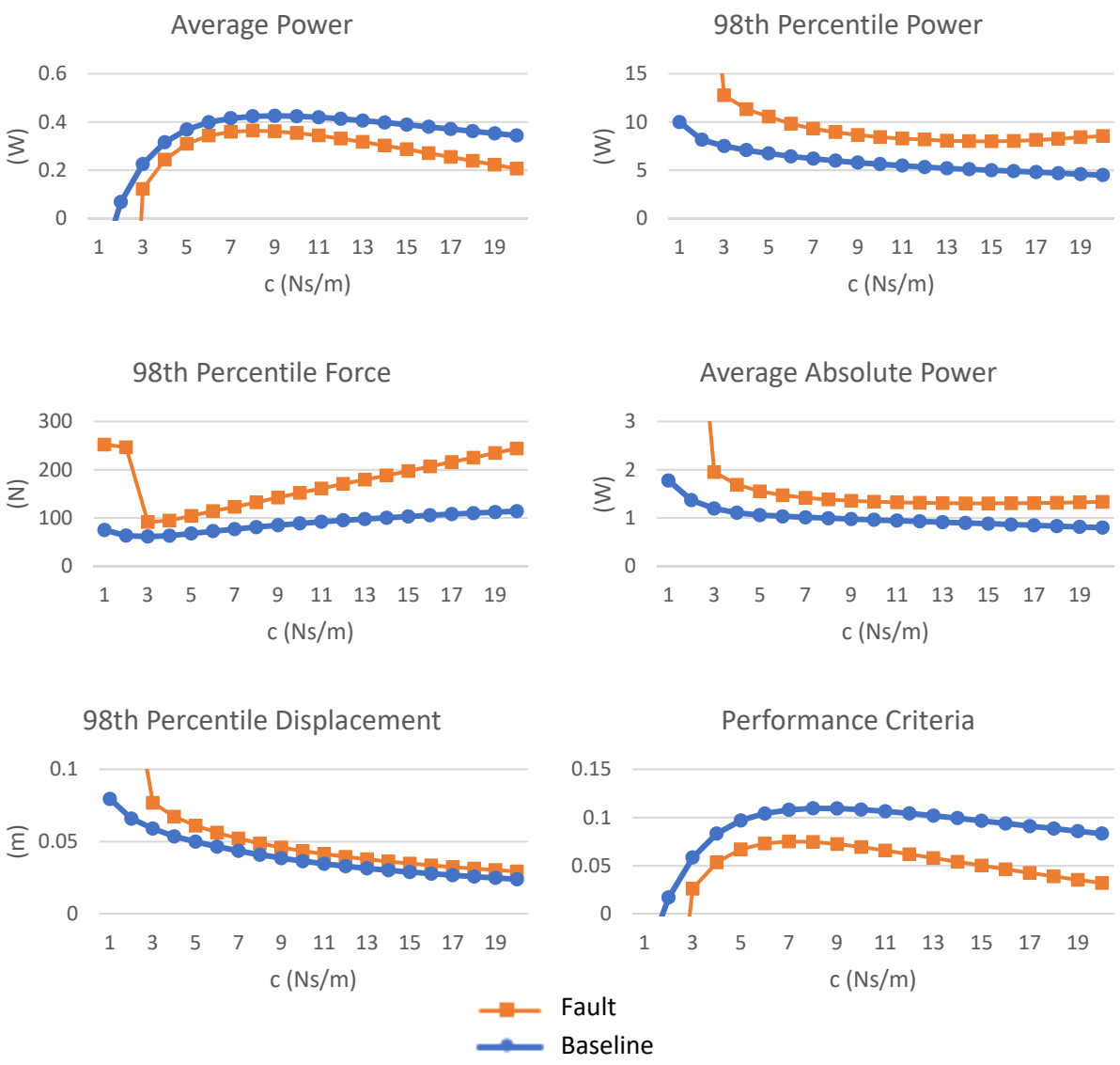

FIG 8. Behavior trends for k = -30 N/m during position sensor signal bias fault in wave state 6

C. Optimal Performance

The overall optimal parameters and maximum achieved performance criterion for each wave state during baseline, position sensor signal bias fault, and position sensor signal scaling fault conditions, are given in Table 2. The controller damping was tested in increments of 1 Ns/m from 0 Ns/m to 20 Ns/m. The controller spring constant was tested in increments of 5 N/m from -5 N/m to -100 N/m.

Table 2. Optimal controller parameters and maximum obtained performance

Wave	Optimal c (Ns/m)			Optimal k (N/m)			Maximum Performance		
State	Baseline	Bias	Scaling	Baseline	Bias	Scaling	Baseline	Bias	Scaling
1	4	4	4	-15	-10	-10	0.00606	0.00545	0.00607
2	6	6	5	-30	-30	-25	0.0563	0.0531	0.0570
3	8	6	7	-35	-25	-30	0.119	0.0839	0.119
4	4	3	3	-15	-10	-10	0.00622	0.00561	0.00624
5	6	6	6	-35	-30	-30	0.0606	0.0569	0.0613
6	9	7	8	-40	-25	-35	0.114	0.0766	0.114

V. CONCLUSIONS & FUTURE RESEARCH

During a fault, the optimal controller parameters are lower than during the baseline case, likely due most to increases in peak commanded controller forces as a result of increases in the peak position signal sent to the controller. During the bias fault, performance decreases significantly even with corrections to controller parameters, while during the scaling fault, the same or slightly higher performance can be obtained with lower magnitude controller parameters. This is likely due to the commanded controller forces being proportional to both the fixed parameters and the position signal received, so that the increase from the scaling fault is offset by the decrease from the varied parameters, resulting in the same forces and thus performance. This offsetting may also explain the improvements in specific elements of the WECs behavior at low magnitude controller parameters during the scaling fault. The slight increases in maximum obtainable performance during the scaling fault in some wave states are most likely due to the large intervals between tested parameter values, so that the true optimal values are not quite obtained.

Future work should include similar comprehensive analyses of behavior during the other faults for which modules were developed, as well as different magnitudes of the faults simulated in this study. Additional faults such as biofouling of submerged and surface components may be modeled. Injection of faults in other WEC devices, such as attenuators and oscillating water columns, could be beneficial and used to identify relative strengths and weaknesses of various WEC types. Such fault injections could also be used to check the robustness of fault-tolerant controllers. Time-series records of forces, displacements, velocities, etc., could be used to develop condition-monitoring systems which may work together with controllers to modify commanded forces either by changing controller parameters or by substituting corrected sensor signals to the controller.

VI. ACKNOWLEDGEMENTS

I would especially like to thank Dr. Yufei Tang and Dr. James VanZwieten of Florida Atlantic University for their guidance and support.

This work was supported in part by the U.S. Department of Energy, Office of Science, Office of Workforce Development for Teachers and Scientists (WDTS) under the Science Undergraduate Laboratory Internship (SULI) program.

VII. REFERENCES

[1] A. Clément et al., “Wave energy in Europe: current status and perspectives, Renewable and Sustainable Energy Reviews, 6(5), 405-431, (2002).

[2] M. Mueller, R. Lopez, A. McDonald, and G. Jimmy, “Reliability analysis of wave energy converters," in *2016 IEEE International Conference on Renewable Energy Research and Applications (ICRERA)*, pp. 667-672. (2016).

[3] Y.-H. Yu, M. Lawson, K. Ruehl, and C. Michelen, “Development and Demonstration of the WEC-Sim Wave Energy Converter Simulation Tool,” in *Proceedings of the 2nd Marine Energy Technology Symposium, METS 2014, Seattle, WA,* (2014).

[4] M. Kramer, L. Marquis, and P. Frigaard, “Performance evaluation of the wavestar prototype,” in *Proceedings of the 9th European Wave and Tidal Energy Conference*, *Southampton, UK* (pp. 5-9), (2011).

[5] E. Balaban, A. Saxena, P. Bansal, K.F. Goebel, and S. Curran, “Modeling, detection, and disambiguation of sensor faults for aerospace applications,” IEEE Sensors Journal, 9(12), pp.1907-1917, (2009).

[6] B. Lu, Y. Li, X. Wu, and Z. Yang, “A review of recent advances in wind turbine condition monitoring and fault diagnosis,” in *2009 IEEE Power Electronics and Machines in Wind Applications,* (pp. 1-7)*,* (2009).

[7] A.B. Sharma, L. Golubchik, and R. Govindan, “Sensor faults: Detection methods and prevalence in real-world datasets,” ACM Transactions on Sensor Networks (TOSN), 6(3), p.23, (2010).

[8] H. Polinder, M.A. Mueller, M. Scuotto, M. and Goden de Sousa Prado, “Linear generator systems for wave energy conversion,” in *Proceedings of the 7th European Wave and Tidal Energy Conference, Porto, Sept.*. (2007).

[9] A. Mérigaud and J. V. Ringwood, “Condition-based maintenance methods for marine renewable energy,” Renewable and Sustainable Energy Reviews, 66, pp. 53-78, (2016)

[10] J.V. Ringwood, et al. "A competition for WEC control systems," in *12th European Wave and Tidal Energy Conference*, (2017).